Journal of Materials Chemistry C

Accepted Manuscript

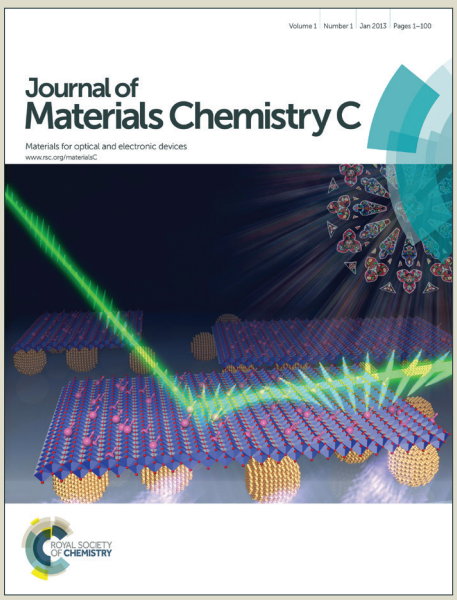

ROYAL SOCIETY OF CHEMISTRY

www.rsc.org/materialsC

Journal Name

RSCPublishing

ARTICLE

The development of artificial porphyrinoids embedded with functional building blocks

Cite this: DOI: 10.1039/x0xx00000x

Zhikuan Zhou and Zhen Shen*

Received 00th January 2012,
Accepted 00th January 2012

DOI: 10.1039/x0xx00000x

www.rsc.org/

In this review article, we summarize the recent advances of artificial porphyrin scaffolds containing various functional building blocks as replacements for pyrrole subunit. These functional moieties are classified into three types: (i) monomeric five/six-membered heterocycles; (ii) linear oligomeric heterocycles; and (iii) aromatic ring-fused heterocycles. The main focus of this article is to compare the influence of these functional building blocks on the photophysical and aromatic properties of the incorporated porphyrinoids. These artificial porphyrinoids are excellent candidates not only for the basic study on the aromaticity of macrocycles, but also for many potential applications such as near-infrared (NIR) dyes, magnetic materials, molecular switches and nonlinear optical materials.

1. Introduction

Natural porphyrins, such as chlorophyll and heme, play important roles in electron transportation and biochemical processes.[1] Porphyrin can be seen as a planar conjugated macrocycle constructed with four pyrrole units that are connected via their α-position by methine carbons. Typically, there are 18 delocalized π-electrons in the conjugation pathway in a porphyrin scaffold. Due to the macrocyclic and aromatic features, porphyrins exhibit distinguished photophysical and chemical properties, such as strong absorption in the UV-visible region, redox interconversion and metal coordination.[2]

To meet the requirements for applications in material science, various synthetic strategies have been employed to construct novel artificial porphyrin homologues, such as *meso*- and β-substitution,[3] ring-contraction[4] and ring-expansion,[5-7] isomerization[8-10] and core-modification,[11] with the main purpose of regulating their structural and electronic properties. Fig.1 shows the representative skeletons of porphyrinoids. From the structural point of view, expanded porphyins, such as sapphyrin, pentapyrin and hexapyrin, can be viewed as the replacement of a pyrrole subunit by a bispyrrole, a dipyrromethene or tripyrrane, respectively. In the case of rubyrin, it can be regarded as the replacement of two pyrrole subunits by two bispyrrole moieties. The conjugation and aromaticity are maintained in the porphyrin-like scaffolds, meanwhile, they possess novel photophysical and electronic properties due to their unique structures.[12] For example, the flexible π-conjugated conformation and large aromatic features of expanded porphyrins exhibit strong absorption and fluorescence in the near-infrared (NIR) region, anion binding property and considerable two-photon-absorption cross-section values,[7] which make them good candidates as NIR dyes, anion probes and non-linear optic materials.[13]

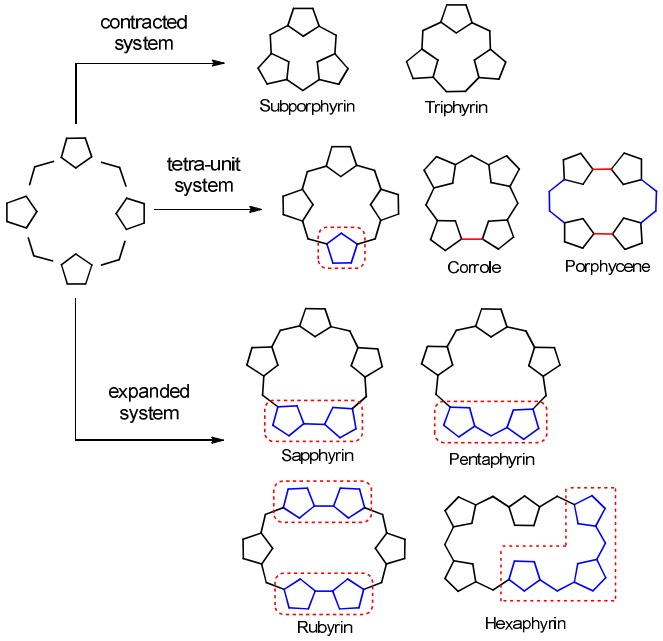

Fig. 1 Representative porphyrin scaffolds. (Pentagons represent five-membered rings such as pyrrole and chalcogen-substituted heterocycles)

In this review article, we regard porphyrin as a scaffold in which one or more pyrrole subunits can be replaced by other five or six-membered rings or small conjugated moieties, which are commonly used in polymer material science. The intriguing structural and electronic properties of these porphyrin-like

networks influenced by the conformation and electronic feature of these functional subunits were summarized. Furthermore, their applications in material science were also reviewed.

2. Porphyrinoids embedded with functional building blocks.

2.1 Synthetic methodologies

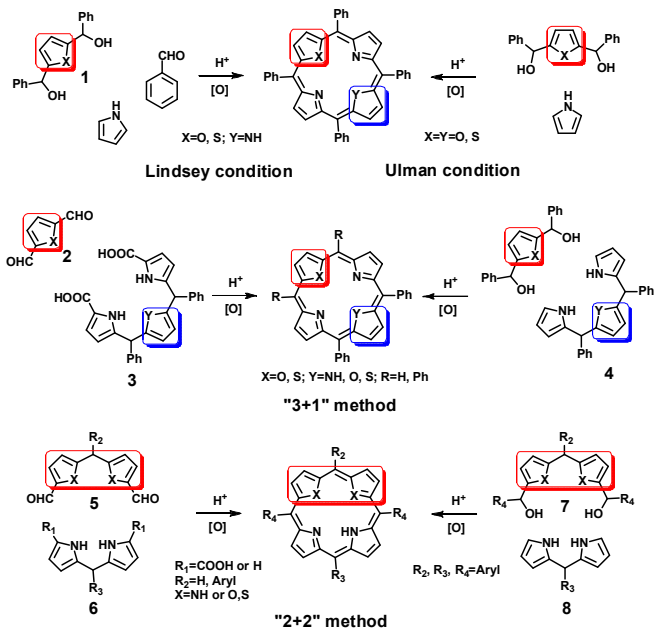

Scheme 1 General synthetic strategies for core-modified porphyrins.

Several synthetic methodologies have been developed since the first artificial porphyrinoid was reported in the early of 20th century. The general synthetic methods include one-pot and stepwise procedures, which were summarized in Scheme 1. Under Lindsey condition,[14] acid catalyzed condensation of pyrrole, aldehyde and diol followed by oxidation with oxidants such as 2,3-dichloro-5,6-dicyano-1,4-benzoquinone (DDQ) or *p*-chloranil, afforded mono-substituted core-modified porphyrins. While Ulman condition[15] provided a facile synthesis of bis-substituted symmetric core-modified porphyrin.

"3+1" method developed by Broadhurst[16] and its modified condition[17] were commonly used for stepwise synthesis of asymmetric porphyrins. Other efficient methods for incorporation of subunits are MacDonald "2+2" type reaction[18] and its modified method.[19] The "1, 2, 3"in the cyclization method refers to the number of heterocycles within the precursors used for acid catalyzed condensation.

From the synthetic point of view, various artificial functional porphyrinoids can be assembled by introducing the functional subunits into diol (**1** and **7**), dialdehyde (**2** and **5**) or tripyrrane (**4**) precursors using the methods described in Scheme 1.

2.2 Building blocks

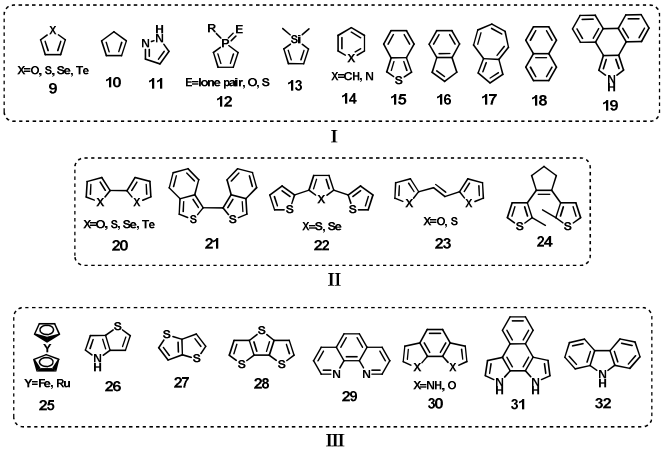

Fig. 2 Structural classification of various building blocks.

Most of the π-conjugated building blocks that are used to permute pyrrole units in a porphyrin skeleton are summarized in Fig. 2. We classified these building subunits into three types based on their structural and electronic features. Type **I** consists of simple five- or six-membered heterocycles. Type **II** are heterocyclic oligomers linked either directly or through bridged atoms such as vinyl group. Type **III** contains heterocycles in ring fused fashion.

Each type of building blocks possesses unique structural and electronic features, which will influence the conformation, photophysical and chemical properties of the incorporated tetra-unit or expanded porphyrin scaffolds.

2.3 Porphyrinoids embedded with type I building blocks.

This type of building blocks consist small five-membered cyclic molecules, such as N-confused pyrrole,[20] chalcogen-containing heterocycles **9**,[21] indene **16** and azulene**17**,[22] or six-membered heterocycles such as benzene and pyridine (Fig. 2). They can be feasibly incorporated into porphyrin and oligopyrrole-like systems and have been extensively studied and reviewed elsewhere.[23] In this section, we mainly focus on the porphyrin skeletons containing some intriguing building blocks in type **I**.

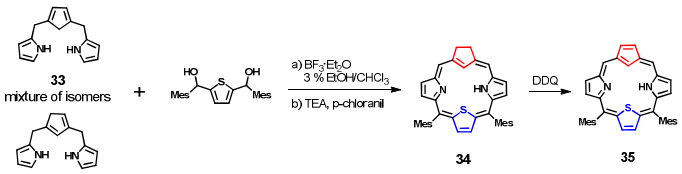

Scheme 2 Synthesis of carbathiaporphyrin **35**. TEA = Triethylamine.

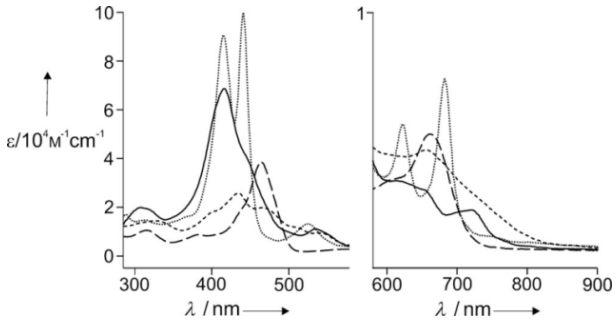

Fig. 3 Absorption spectra of **34** (solid line), **35** (dotted line), **34-Pd** (short dashed line), and **35-Pd** (long dashed line) in CH_2Cl_2. Reproduced from Ref. 22 with permission from Wiley.

Recently, Latos-Grażyński*et al.* reported acabathia-porphyrin **35** containing cyclopentadiene subunit (Scheme 2).[24] **35** was prepared by [3+1] condensation of a mixture of isomeric tripyrrane **33** and thiophenediol. After first oxidation with *p*-chiloranil, a stable aromatic chlorine-like derivative **34** was obtained, further carefully oxidation with one equivalent of DDQ yield the target 18-π cabathiaporphyrin **35**. **34** exhibits a relatively broad Soret band at 417 nm, while **35** displays splitted Soret bands at 415 and 441 nm (Fig.3, left). Both compounds are aromatic with a set of weak Q bands (Fig.3, right). Their Pd-complexes **34-Pd** and **35-Pd** were investigated for the first time which showed distinct change in the absorption spectra. The N2SC core based on the existence of cyclopentadiene make porphyrins **34** and **35** excellent macrocyclic ligands to coordinate with various metal ions like other cabaporphyrins.[25]

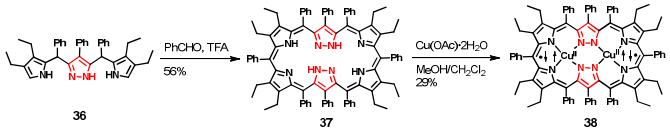

Scheme 3 Synthesis of expanded porphyrin **37** and its dicopper complex **38**.

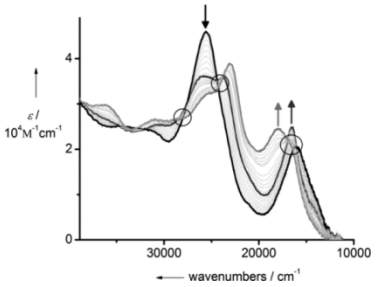

Fig. 4 UV-Vis-NIR absorption spectra of **38** recorded during electrochemical oxidation in CH_2Cl_2, **38** (black line), $[\mathbf{38}]^+$ (dark gray line), and $[\mathbf{38}]^{2+}$(light gray line) are highlighted. Isosbestic points are indicated via black circles. Adapted with permission from Ref 27. Copyright 2013 American Chemical Society.

Inspired by the excellent ability to provide polydentate binding sites as bridging ligands in multinuclear transition metal complexes, Meyer *et al.* employed pyrazole[26] as a building block to construct hexaphyrin-like[27] expanded porphyrin framework **37** (also called Siamese-twin porphyrin).[28] **37** was synthesized in satisfactory yield through Lindsey type cyclization of pyrazole-containing tripyrrane **36** and benzaldehyde. The ingenious design resulted in two adjacent tetraporphyrin-like coordination cavities in one skeleton, although the entire macrocycle showed non-aromatic properties due to the broken π-conjugation pathway at the pyrazole units. Stable dicopper(II) complex **38**[29] was prepared, which can be easily converted to $[\mathbf{38}]^{2+}$ by oxidation with $AgBF_4$ or electrochemical procedure (Fig. 4). As revealed by X-ray analysis, two-fold oxidized $[\mathbf{38}]^{2+}$ adopted similar twisted helix fashion structure with **38**, in which two copper were tetragonal coordination. $[\mathbf{38}]^{2+}$ is a ligand-centered radical species with invariant copper oxidation state (Scheme 3). Electronic interaction between two copper in close proximity combined with the impact of potentially noninnocent expanded porphyrin ligand made **38** a valuable platform with rich redox chemistry, which may find application in bioinspired multi-electron processes.

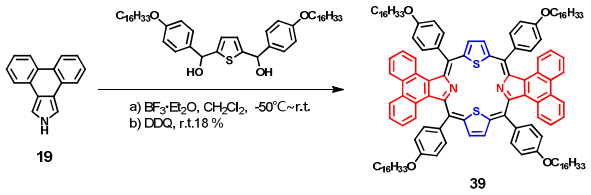

Scheme 4 Synthesis of dithio-core-modified phenanthroporphyrin **39**.

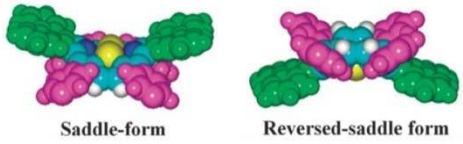

Fig. 5 Tentative conformations of saddle-shaped and reversed-saddle-shaped architectures of **39** on pyrolytic graphite surface. Reproduced by permission of the PCCP Owner Societies.

Shen *et al.* have employed phenanthrene ring fused pyrrole **19** to increase the rigidity and π-conjugation in BODIPY and porphyrin molecules.[30, 31] They successfully synthesized core-modified porphyrin **39** by the condensation reaction of pyrrole **19** and thiophenediol using Ulman method [15] in 18 % yield.[32] The incorporation of phenanthrene fused pyrrole efficiently extended the π-conjugation of porphyrin and redshifted its Soret and Q bands to 514 and 837 nm in $CHCl_3$, respectively. Moreover, the emission band of **39** centered at λ > 900 nm. The build-in phenanthrene fused pyrrole moieties caused considerable steric hindrance with the *meso*-phenyl substituents, thus force the π-system to adopt a heavily distorted saddle-like structure. Zeng and Shen *et al.* further investigated the 2D self-assembly behavior of **39** on a highly-oriented pyrolytic graphite (HOPG) surface by high-resolution STM.[33] Interestingly, when **39** was added into a non-polar solvent, such as *n*-tetradecane and 1-phenyloctane, the macrocycle framework assembled into a saddle-form architecture, while in polar solvent, such as

heptanoicacid, the conformation is totally reversed (Fig. 5). The results showed that core-modified porphyrin embedded with phenanthrene fused pyrrole may form highly ordered 2D network in solid-liquid interface, which made it possible to fabricate porphyrin-based devices.

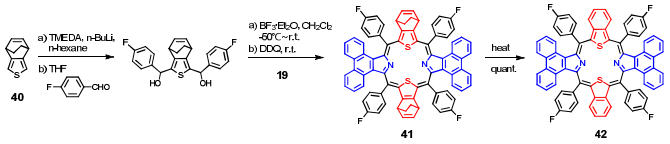

Scheme 5 Synthesis of core-modified porphyrin **42** embedded with isothianaphthene **15**.

Isothianaphthene (ITN, or benzo[*c*]thiophene, **15**) is a widely used precursor for small bandgap linear π-conjugated polymers[34] due to its contribution to π-extension. The poor stability and complicated synthetic procedure have impeded its application until Ono *et al.*[35, 36] reported a facile and efficient retro-Diels-Alder strategy, in which soluble bicyclo[2.2.2]octadiene (BCOD) thiophene **40** precursor was employed to convert into ITN quantitatively by heating under vacuum. As shown in Scheme 5, Shen *et al* reported the reaction of lithium salt of **40** with *p*-fluorobenzaldehyde to give its diol compound which condenses with phenanthrene fused pyrrole **19** to form soluble porphyrin **41**.[32] Core-modified porphyrin **42** embedded with both ITN and phenanthrene-fused pyrrole subunit was successfully synthesized from **41** by heating at 300°C under vacuum quantitatively. The aryl-fused thiophene and pyrrole units in **42** extended the π-conjugation of normal porphyrin thus showed redshifted Soret band at 543 nm and Q bands at 712 and 866 nm, made it possible for application as near IR dyes.

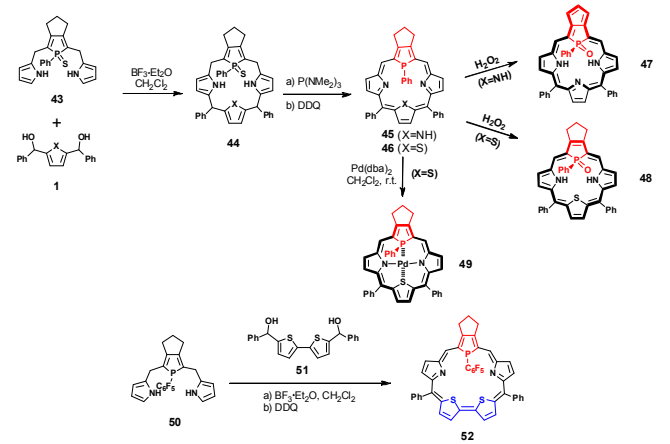

Scheme 6 Synthesis of phosphaporphyrins **47**-**49** and **52**.

In addition to carbon and chalcogen atoms, other elements such as phosphorus and silicon have been employed to replace the core nitrogen atoms of porphyrins to perturb their electronic structures. Imahori*et al.* successfully introduced phosphole unit into porphyrin to obtain phosphaporphyrins **45** and **46**.[37, 38] The key synthon P-masked phosphatripyrrane **43** was synthesized through a carefully designed route, which was condensed with thiophene or pyrrolediol compound **1** under $BF_3{\cdot}Et_2O$ catalyzed [3+1] condition to afford porphyrinogen **44**. After desulfurization with $P(NMe_2)_3$ and oxidation with DDQ, **45** and **46** were obtained as stable solids which slowly decomposed in solution when exposed to air and light. The durability of the +3 valence state P center to acid and oxidant were dramatically improved through introduction of electron-withdrawing pentafluorophenyl group onto the phosphorus atom. It was revealed that expended phosphaporphyrins **52** was chemically stable and structurally rigid with only slightly perturbed aromaticity and electronic properties (Scheme 6).[39]

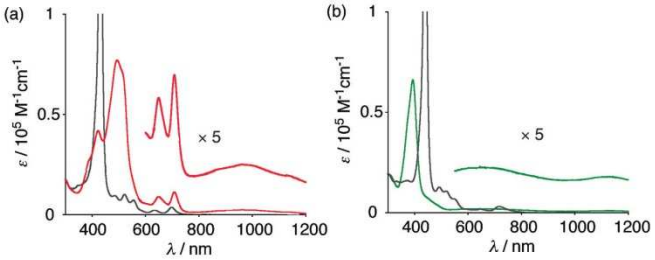

Fig. 6 UV-vis absorption spectra of **47** (a, red) and **48** (b, green).The spectra of **45** and **46** were shown in black lines in a and b, respectively. Reproduced with permission from Ref. 36. Copyright 2010 American Chemical Society.

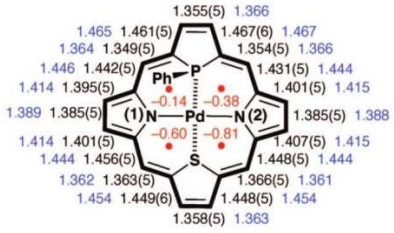

Fig.7 Bond lengths of **49** determined by X-ray (black) and DFT calculation (blue), NICS values (red). Adapted with permission from Ref. 39. Copyright 2008 American Chemical Society.

Relatively smaller HOMO-LUMO band gaps were found for phosphaporphyrins **45** and **46** compared with regular porphyrins. Thus, they showed redshifted Soret and Q-bands (**45**: 431 and 698 nm; **46**: 440 and 718 nm). The phosphorus center in phosphole unit can be easily functionalized by oxidation, substitution or complexation with metal ions such as Ni^{2+}, Pd^{2+} and Pt^{2+}.[40] Unique aromaticity switching properties were found for both 18-π aromatic **45** and **46** by oxidation with H_2O_2 (Scheme 6). The fused cyclopentane subunit and phosphorus center of phosphole were oxidized to cyclopentadiene and phosphoryl, respectively, which resulted in the extension of π-conjugation pathway of **45** and the formation of a 22-π aromatic system **47**. While in the case of **46**, oxidation only occured at phosphorus center, thus afforded a 20-π antiaromatic system **48**.[38] The aromatic **47** showed split Soret bands at 422 and 494 nm with broad Q band at 964 nm, while antiaromatic **48** exhibited high-energy region absorption band at 394 nm and no obvious Q band (Fig. 6). Furthermore, due to the high affinity between P and metal atoms, complexation of

46 with zero valence group 10 metals afford stable 20-π antiaromatic isophlorin complexes **49**. Alternative single-double bond derived from X-ray data combined with DFT calculation and nucleus-independent chemical shifts (NICS) value[41, 42] (close to zero, Fig.7), clearly demonstrated the antiaromatic properties of Pd complex **49**. [43]

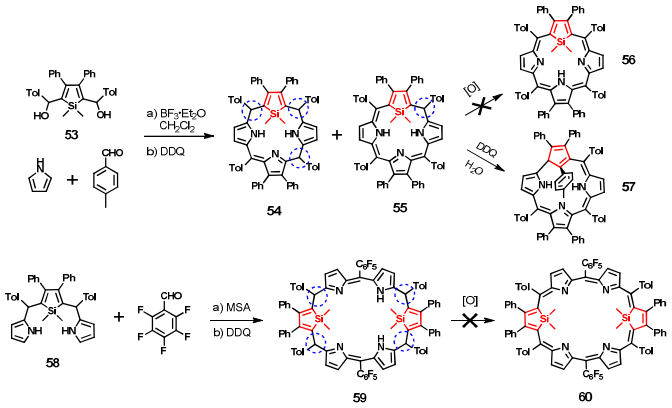

Scheme 7 Synthesis of porphyrinoids containing silole units.

Scheme 7 showed two examples of attempt to synthesize porphyrinoids **56** and **60** that embedded with silole **13** moieties. Through a one-pot reaction of silolediol **53**, pyrrole and *p*-tolylaldehyde catalyzed by $BF_3{\cdot}Et_2O$ and oxidation by DDQ subsequently, only small amount of phlorin-like compounds **54** and **55** were obtained.[44] Further oxidation with DDQ resulted in the formation of an unexpected *iso*-carbacorrole **57** rather than the desired porphyrin-like product **56**. Coordination with Cu and Ag converted non-aromatic *iso*-carbacorrole **57** into its complexes that were aromatic. Methane sulfonic acid (MSA) catalyzed condensation of silatripyrrane **58** and pentafluorobenzaldehyde followed by oxidation with DDQ generated a stable hexaphyrinoid **59** instead of the desired macrocycle **60**.[45] Although conjugated porphyrin-like macrocycles embedded with silole were not trapped, the above results presented detailed studies on the reactivity of silole within porphyrin environment.

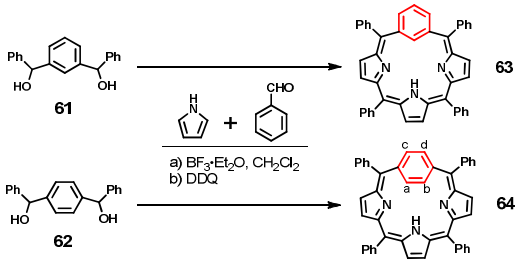

Scheme 8 Synthesis of benziporphyrins **63** and **64**.

Six-membered rings such as benzene and pyridine are typical 6-electron aromatic molecules. When introduced into a porphyrin framework, their local aromaticity usually impedes the global π-conjugation of the macrocycles. For example, in benziporphyrin **63**,[46, 47] benzene unit was linked with the tripyrrolic brace through 1, 3-position, this resulted in the loss of π-electron delocalization in the whole molecule which turned out to be non-aromatic. By changing the connection fashion of benzene into 1,5-position (Scheme 8), an aromatic benziporphyrin **64** was achieved.[48] The chemical shifts of inner CH protons a and b appeared at upper-field 2.32 ppm, while the out ones c and d at 7.68 ppm (168K), clearly demonstrated the existence of a diatropic ring current. These results were consistent with the observed reduction of bond lengths of phenylene subunit (1.365-1.390 Å). Similar phenomenon that different build-in manners of subunits lead to distinct diversity of properties was also found in porphyrin embedded with naphthalene **18**.[49, 50]

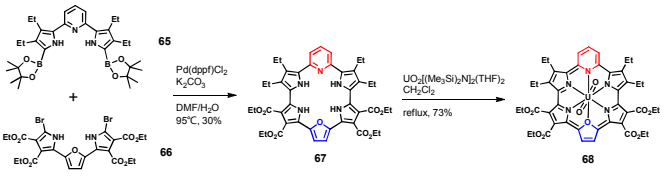

Scheme 9 Synthesis of expanded porphyrin **67** and its uranyl complex **68**.

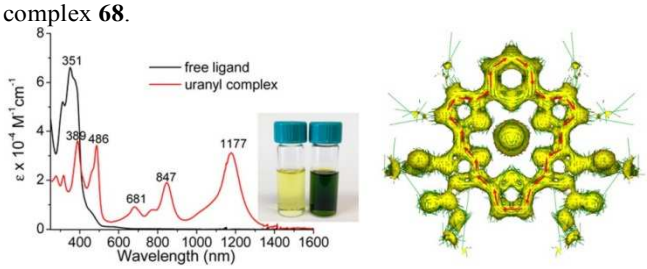

Fig. 8 Left: UV-Vis spectra of **67** and **68** in CH_2Cl_2; right: ACID plot of **68**. Adapted with permission from Ref. 47. Copyright 2014 American Chemical Society.

Recently, Sessler *et al* reported the construction of a pyridine-containing expanded porphyrin **67** through Pd(II)-catalyzed Suzuki coupling of 2,6-dipyrrolylpyridine diborate **65** and dibromo compound **66** in 30% yield (Scheme 9).[51] The absorption of this macrocycle showed high-energy Soret-like band at 351 nm without obvious Q band, which indicated its non-aromatic feature. Interestingly, upon complexation with large uranyl cation, the dianionic form of **67** was stabilized and an aromatic complex **68** was achieved. Two sharp Soret-like bands at 389 and 486 nm accompanied by three Q-like bands at 681, 847 and 1177 nm demonstrated its aromatic feature. Anisotropy of the induced current density (ACID)[52, 53] plot of **68** exhibited a diatropic ring current (Fig. 8, clockwise, red arrows) around the macrocycle, clearly supported the fact that complexation with anion increased the aromaticity of macrocycle.

2.4 Porphyrinoids embedded with type II building blocks.

The type **II** building blocks in Fig. 2 are composed of two or more five-membered heterocycles that are linked at α or β position directly (**20-22**) or by unsaturated bridges (**23**, **24**). Permutation of pyrrole units in normal porphyrin by these larger-size subunits usually leads to the expansion of porphyrin framework into sapphyrin-, rubyrin- or hexaphyrin-like

macrocycles. These functional subunits incorporated expanded porphyrins have more attractive properties than normal tetrapyrrole porphyrins such as absorption and fluorescence in the near-infrared (NIR) region, better anion binding ability, flexible structure and aromatic switching.

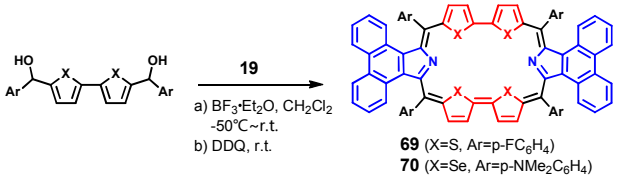

Scheme 10 Synthesis of core-modified rubyrins **69** and **70**.

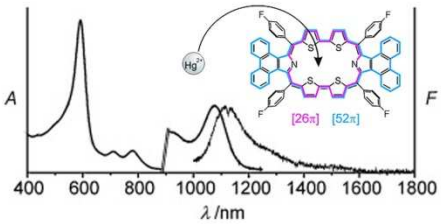

Fig. 9 Absorption and emission spectra of **69** in $CHCl_3$. (λ_{ex} = 532 nm). Inset shows two conjugation pathways in **69**. Reproduced from Ref. 49 with permission from Wiley.

Bithiophene is a commonly used building block to extend conjugated framework of porphyrin into rubyrin which showed red-shifted absorption and better anion binding property.[54] Shen *et al*. reported a core-modified rubyrin **69**[55] with build-in bithiophene **20** and phenanthrene-annulated pyrrole **19** (Scheme 10). Ring fusion led to a cross-conjugated 26- and 52-π hexaphyrin **69**, which displayed a Soret band at 596 nm and three Q bands at 714, 784 and 1076 nm (Fig. 9). The steric hindrance between phenanthrene-annulated pyrrole and peripheral fluorophenyl groups forced rubyrin **69** to adopt a bowl-shaped structure, which effectively prevents self-aggregation. Simple test strips that were made by embedding **69** into a polyurethane membrane were used for rapid Hg^{2+} screening in aqueous solution.

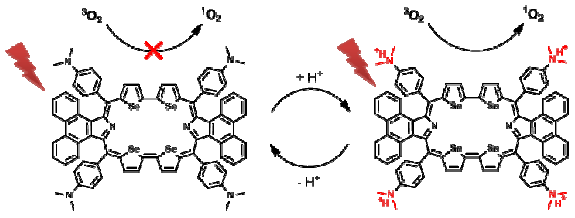

Fig. 10 Structure and function of pH-activatable **70** for $^1O_2$ generation. Adapted with permission from Ref. 50. Copyright 2013 American Chemical Society.

By using the same strategy, biselenophene unit was introduced into a porphyrin skeleton to form rubyrin **70**[56] with near-infrared absorption and emission. Due to the heavy atom effect, the selenium atom enhanced the $^1O_2$ generation efficiency, meanwhile, the peripheral dimethylaminophenyl groups led to the pH-controllable activation of **70** (Fig. 10). High singlet oxygen quantum yield (Φ_Δ) was obtained under NIR irradiation (635 nm) at acidic condition (Φ_Δ=0.69, pH=5.0), while **70** was deactivated at physiological pH (Φ_Δ=0.06, pH=7.4). The **70**-loaded nanoparticle functionalized with cancer cell-targeting reagent folate was designed and used as an acidic pH-activatable targeted photosensitizer for selective NIR photodynamic therapy against cancer.[56]

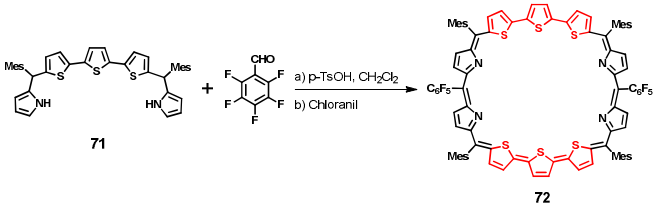

Scheme 11 Synthesis of core-modified rubyrin **72**.

Expanded porphyrin **72** which contains two terthiophene units **22** has been synthesized via an *p*-methylbenzene sulfonic acid catalyzed [5+5] MacDonald condensation of modified pentapyrrane **71** and pentafluorobenzaldehyde (Scheme 11).[57] The increase in the number of thiophene unit extended the π-conjugation. Macrocycle **72** possessed planar conformation and exhibited high two-photo absorption cross-section value of 108000 GM with respect to Rhodamine-6G reference, which made it possible for applications in the field of nonlinear optical devices.

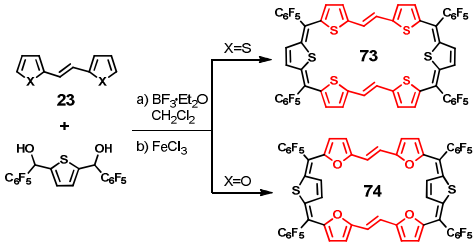

Scheme 12 Synthesis of vinylogous expanded isophlorins **73** and **74**.

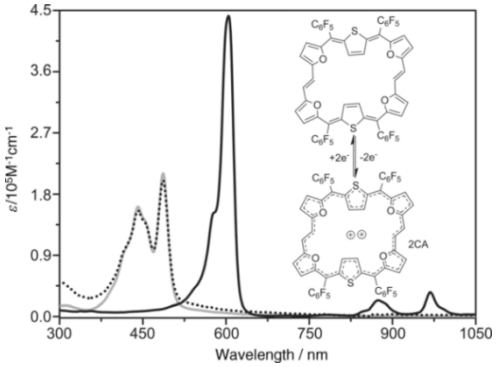

Fig. 11 Changes in the UV/Vis absorption spectra of **74** (gray solid line) upon addition of TFA (black solid line) followed by triethylamine (dotted line). CA = $[CF_3COO]^-$. Adapted from Ref. 53 with permission from Wiley.

In planar or near-planar conjugated systems, aromaticity and antiaromaticity were determined via Hückel's (4n+2) and 4n π-electron rule. Altering the number of building blocks or the

connection pattern between them is a widely used method to tune the number of π-electrons in conjugated macrocycles. E-ethylene bridged bis(thiophene)/furan **23** were employed to synthesize two stable antiaromatic 32π expanded isophlorin **73**[58] and **74**[59] (Scheme 12). The crystal structure analysis of **73** revealed that there were unprecedented intermolecular F···S, C-H···F and π-π interactions which are very rare for antiaromatic system. With four furan rings, **74** adopted ring-inverted conformation. In the neutral form, **74** exhibited split Soret band at 430 and 482 nm without obvious Q-like bands, while upon addition of TFA or oxidant such as [$Et_3O^+SbCl_6^-$], the Soret band redshifted to 580 and 611 nm accompanied by appearance of two Q bands between 800 to 1000 nm. Triethylamine or reductant such as $FeCl_2$ could reduce the dication form of **74** to its neutral form (Fig. 11). ^{1}H NMR confirmed the reversibility between 4n π and (4n+2) π states of **74** by suitable redox conditions.

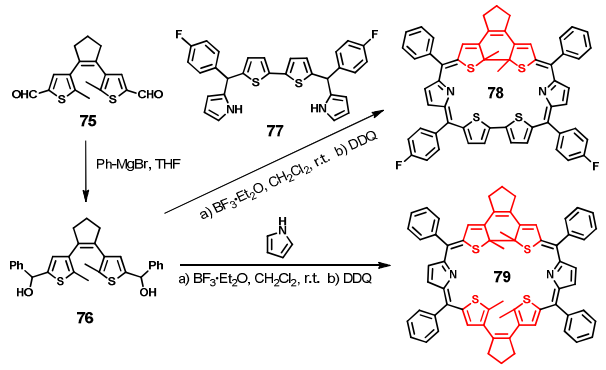

Scheme 13 Synthesis of dithienylethene containing core-modified rubyrins **78** and**79**.

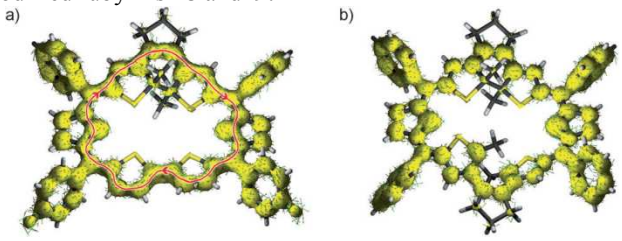

Fig. 12 ACID plots of **78** (a) and **79** (b) at an isosurface value of 0.065. Reproduced from Ref. 56 with permission from Wiley.

Another possible way to tune the aromaticity of porphyrinoid is to incorporate stimuli-responsive building blocks into porphyrin skeleton. Dithienylethene **24** is an excellent candidate which exhibit switchable open-closed conformation interconversion in response to light or certain redox potential.[60, 61]Core-modified rubyrins which contain one and two dithienylethene moieties **78** and **79** were synthesized starting from the corresponding diol compound of **24** via [4+1] and Ulman condition[62], respectively (Scheme 13). Probably due to the ring strain, the dithienylethene unit in aromatic **78** adopted a closed-form conformation, while in non-aromatic **79**, one of the two dithienylethene units adopted an open-form conformation which was confirmed by X-ray analysis, NMR and UV-Vis spectrum. ACID plot of **78** showed a clear clockwise ring current which indicated the 26π aromatic feature of the conjugated system. In contrast, no obvious ring current was found along the outer ring periphery of **79** (Fig. 12). The structure of dithienylethene does have an impact on the aromaticity of macrocycles, it is possible to construct proper conjugated porphyrinoids with build-in dithienylethene moieties to form stimuli-active molecules for applications in molecule switch.

2.5 Porphyrinoids embedded with type III building blocks.

The type **III** building blocks in Fig. 2 are composed of two or more five or six-membered heterocycles that are connected in fused fashion. From the structural and synthetic point of view, it is possible to embed these building blocks into tetra-unit or expanded porphyrin skeleton. All these building blocks are π-conjugated molecules with rigid conformation which have the ability to extend the π-conjugation of porphyrinoids and increase their structural rigidity. Some of them possess unique electronic structure that may perturb the conjugation pathway of porphyrinoids when incorporated into their framework (such as **25-26**). **29-32** contain fused benzene or pyridine unit, it is fascinating to investigate the global electronic property of porphyrinoids that embed with these subunits having local π-conjugations.[63]

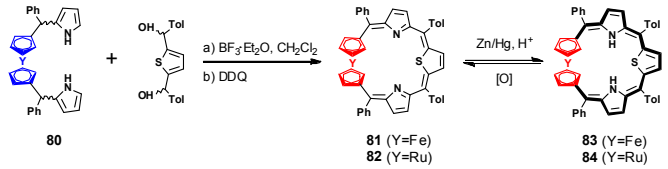

Scheme 14 Synthesis of core-modified porphyrins **81** and **82** embedded with ferrocene and ruthenocene.

As a pioneering work, Latos-Grażyński *et al* employed core-modified porphyrin as a platform to investigate the electronic conjugation across metallocene in a fully conjugated macrocycle. Ferrocenothiaporphyrin **81**[64] and ruthenocenoporphyrin **82**[65], which possess a build-in ferrocene and ruthenocene unit, respectively, were synthesized via [3+1] cyclization reaction (Scheme 14). Distorted conformation of both **81** and **82** were demonstrated by X-ray structure analysis. ^{1}H NMR data revealed the antiaromatic nature of molecules **81** and **82**, while their two-electron reduced congeners **83** and **84** showed clear aromatic properties. It provided a possibility that the macrocyclic π conjugation can transmit across a d-electron metallocene to form a three-dimensional aromatic system.

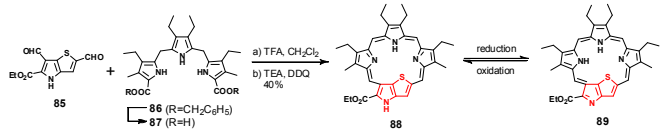

Scheme 15 Synthesis of heteroporphyrin **88** containing thienopyrrole unit.

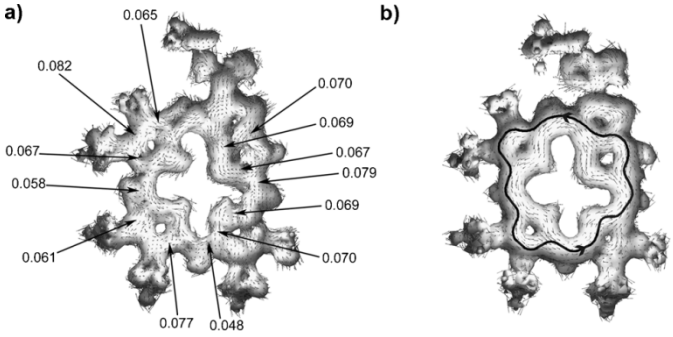

Fig. 13 ACID plots of a) **88** and b) its tautomer **89** at an isosurface value of 0.03. The external magnetic field is applied orthogonal to the macrocycle plane with its vector pointing towards the viewer. Current density vectors (lines and conics) are plotted onto the ACID isosurface. The critical isosurface values (CIV) for compound **88** are provided. Reproduced from Ref. 61 with permission from Wiley.

Shen *et al.* reported a heteroporphyrin **88**[66] embedded with a thienopyrrole unit through TFA-catalyzed condensation of dialdehyde **85** with reactive diacid **87**[67] which was prepared in situ from debenzylation of **86** by catalytic hydrogenation (Scheme 15). **88** exhibited a near-planar conformation in the solid state. The relatively broad absorption bands at 356 nm and 455 nm changed into an intense peak at 410 nm accompanied by several weaker bands between 500-800 nm upon reduction by $NaBH_4$ or a controlled electrochemical reduction at potential E_{app} = -1.35V. Due to N-H tautomerism, the thienopyrrole unit acted as a switch to tune the aromaticity of heteroporphyrin between the stable nonaromatic **88** and 20π antiaromatic **89** under proper redox condition. The ACID isosurface plot for **88** predicted relatively poor electron conjugation, as there is a disrupted pattern within the electronic current. Its tautomer **89** contains counterclockwise currents, which means a stronger antiaromatic ring current is generated in the tautomer that has a 20 π-electron conjugation system. (Fig. 13)

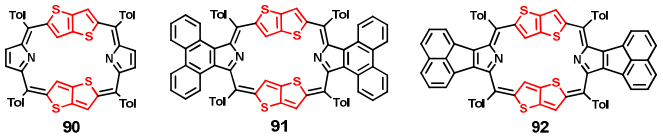

Scheme 16 Structures of heteroporphyrins **90-92** containing thienothiophene unit.

Three heteroporphyrins that contain thienothiophene as building blocks were reported. **90-92**[68] are 22π aromatic macrocycles (Scheme 16). Annulated pyrroles in **91** and **92** contributed to the delocalization of π electrons and thus redshifted their Soret band for 56 nm compared to **90**. Compound **90** showed a Soret band at 503 nm with a shoulder at 530 nm, followed by an intense Q-band at 725 nm and other two broad Q-bands at 868 nm and 957 nm. **91** showed an intense Soret band at 559 nm with three relatively weak Q-bands at 656 nm, 719 nm and 973 nm. **92** exhibited almost the same absorption peak pattern as **91**. The absorption of these thienothiophene-containing heteroporphyrins well extend into the NIR region.

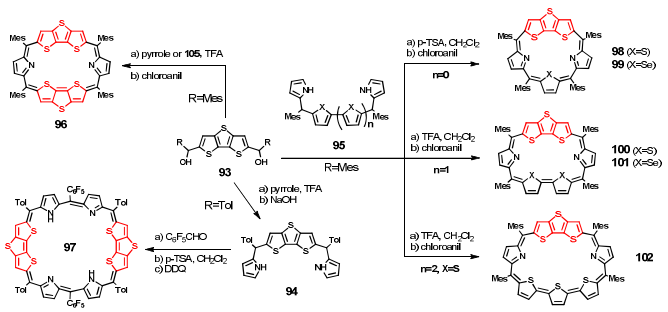

Scheme 17 Synthesis of heteroporphyrins **96-102** embedded with dithienothiophene unit.

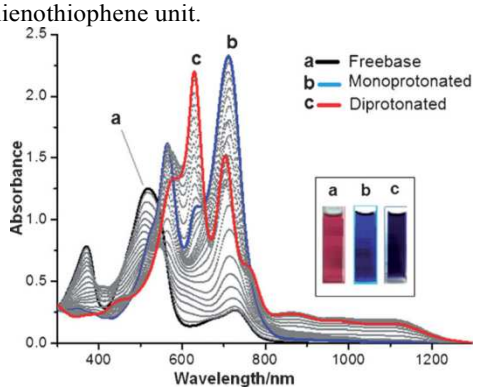

Fig. 14 Titration of TFA (0.1-100 mM) to **97** (0.01 mM) in CH_2Cl_2. Reproduced from Ref. 68 with permission from Wiley.

Dithieno[3,2-*b*:2',3'-*d*]thiophene (dithienothiopheneor DTT) **28** is a widely used building block in conjugated polymers for application in electronic and photovoltaic devices.[69, 70] As a condensed and fused structure of thiophene, DTT can be introduced into porphyrin skeletons of various ring size via its diol compound **93** (Scheme 17). Four, five and six-unit heteroporphyrins **96**, **98-102**[71, 72] embedded with rigid DTT moiety exhibited more planar and rigid conformations and enhanced aromaticity compared with their bithiophene congeners. Structural diversity was found for **99**, in which the selenophene ring switched between the normal and inverted form in the free base and protonated condition, respectively.[72] Due to the structural flexibility of dipyrin linkage in the same macrocyclic networks, 36π nonaromatic **97**[73] adopted a figure-eight twisty conformation in the solid state. Upon stepwise protonation by TFA, monoprotonated **97** showed a Soret-like band at 568 and weak Q bands at 816 and 1136 nm. Further protonation leaded to diprotonation resulting in two sharp Soret-like bands at 632 and 701 nm followed by broad absorption between 800-1200 nm (Fig. 14). These observations were consistent with the structural changes from figure-eight to near-planar in the solid state upon protonation.

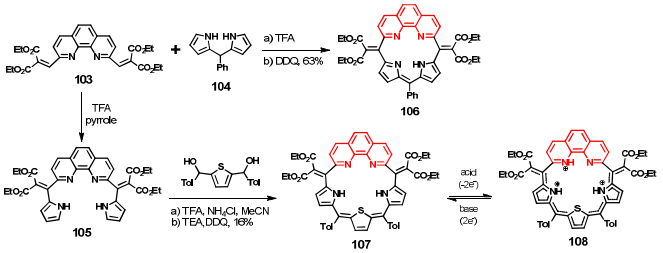

Scheme 18 Synthesis of porphyrin-related macrocycles **106** and **107** embedded with 1,10-phenanthroline moiety.

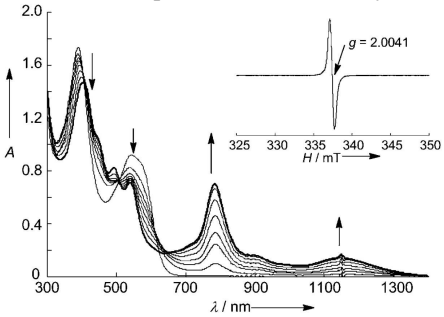

Fig. 15 UV/Vis-NIR spectroscopic changes of **107** upon titration withTFA in $CHCl_3$ ([**107**]=4×10^{-5}M). Inset shows the solid ESRspectrum of **107**·3TFA at room temperature.Reproduced from Ref. 71 with permission from Wiley.

Naruta *et al* reported a porphyrin-like macrocycle **106**[74] embedded with a 1,10-phenanthroline subunit **29** (Scheme 18). The *meso*-alkylidenyl double bonds are of great importance for the stabilization of the nonaromatic macrocycle system.[75] Phenanthroline in the structurally flexible **106** provide two juxtaposed neutral nitrogen binding sites for smaller Mg^{2+} ion. In 0.1M HEPES buffer (DMSO/H_2O=7:3 v/v, pH 7.4), both the absorption and emission band of **106** redshifted from 496 to 575 nm and from 583 to 631 nm upon addition of Mg^{2+}, respectively. Moreover, the binding constant of **106**-MgCl complex was found to be K_{Mg}=37.3M^{-1} even in the presence of water, which made **106** an excellent candidate for assessing the total content of cellular Mg^{2+}. Further study on the incorporation of **29** into a larger sappyrin-like platform yield macrocycle **107**[76] (Scheme 18). The crystal structure of **107** showed severe distortion. Upon addition of TFA or trichloroacetic acid, an intense absorption at 766 nm accompanied by a broad band extending to 1400 nm appeared (Fig. 15). This implies the protonation-induced alteration of the macrocyclic π-conjugation. Unprecedentedly, closed-shell molecule **107** was transformed into a stable biradicaloid species **108** upon protonation by acid with an ESR signal centered at g=2.004 (Fig. 15). This interesting finding offers an important opportunity for exploitation of molecule-based magnetic materials.

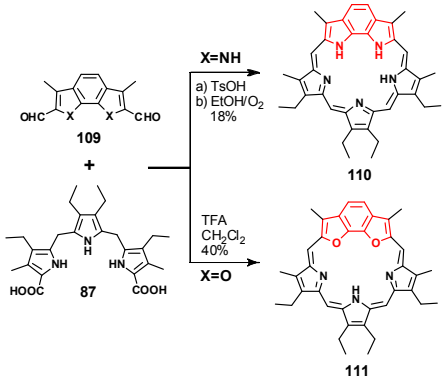

Scheme 19 Synthesis of sapphyrins **110** and **111** embedded with benzodipyrrole or benzodifuran moiety.

Benzodipyrrole and benzodifuran **30** were embedded into sapphyrin skeleton through [3+1] condensation from their diformylated derivatives **109** and tripyrromethane dicarboxylic acid **87**, respectively (Scheme 19). ^{1}H NMR analysis revealed that the inner NH protons of **110**[77] resided unsymmetrically as shown in Scheme 19. Free-base **110** showed a broad Soret-like band at 466 nm and a Q-band at 727 nm, which appeared as an intense peak at 469 nm with a major Q-band at 703 nm upon diprotonation with *p*-toluene sulfonic acid. It appeared that incorporation of the benzodipyrrole unit increased the rigidity of sapphyrin network and had a strong influence on the electronic properties of the molecule. Sessler *et al*. incorporated benzodifuran subunit into a sapphyrin system **111**[78] and examined its anion binding properties. Diprotonated form of dioxabenzosapphyrin **111** was found to bind fluoride and chloride anions only weakly in MeOH. Meanwhile, molecular recognition behavior that interacted with neutral Ar-OH species was also observed.

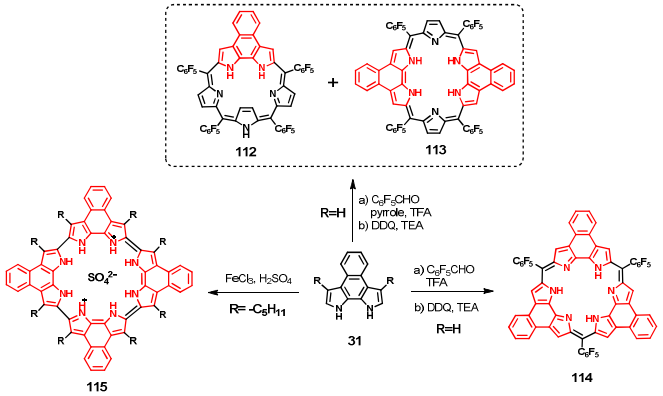

Scheme 20 Synthesis of expanded porphyrins **112-115** embedded with naphthobipyrrole moiety.

1,10-dihydrobenzo[*e*]-pyrrolo[3,2-*g*]indole **31** (also termed as naphthobipyrrole) was a rigid and conjugated building block that is composed of a naphthalene and two fused pyrrole units. Due to the existence of two unsubstituted pyrrole α-position, naphthobipyrrole can be introduced into expanded porphyrin system by using the same synthetic method as for pyrrole.

Scheme 20 shows the preparation and structures of a series of porphyrinoids with one to four build-in naphthobipyrrole moieties. The incorporation of napthobipyrrole units imposed an conformational restriction on the porphyrin skeleton. One of the pyrrole rings adopted an inverted conformation in the free-base form of sapphyrin-like macrocycle **112**[79]. Upon mono-protonation by TFA, the inverted pyrrole transformed into normal "NH in" conformation, whereas diprotonation caused re-inversion of the pyrrolic subunit. Rubyrin-like **113**[79] exhibited spectroscopic properties consistent with aromatic 26π system. Its mono-HCl salt possessed a nearly planar conformation in the solid state. 30π aromatic cyclo[4]naphthobipyrrole **115**[80] was obtained as a dihydrogen sulfate salt via an $FeCl_3$-oxidized cyclization of the alkyl-substituted naphthobipyrrole.[81] The crystal structure analysis revealed that **115** adopted a saddle-type conformation. The Q-band of **115** extended well into NIR region (1276 nm) with high extinction coefficient (2.19×10^5 $M^{-1}cm^{-1}$). Interestingly, **115** showed large two-photo absorption cross section values ($3.3\text{-}5.2\times10^4$ GM) in 600-800 nm range, which made it a promising pigment for application in nonlinear optic devices.[82]

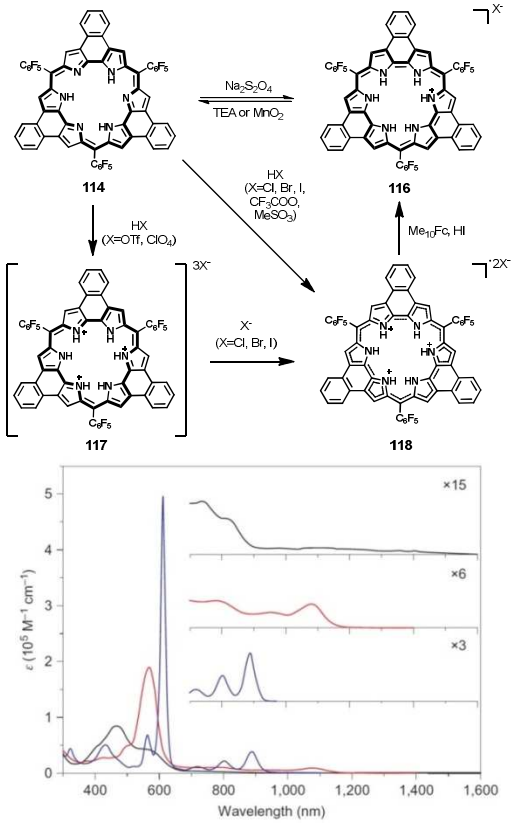

Fig. 16 a) Redox reaction cycle of **114** observed in the presence of protic acids and an organic base. b) Steady-state absorption spectra of compounds **114** (black line),**118** (red line) and **116** (blue line) in CH_2Cl_2. Reprinted by permission from Macmillan Publishers Ltd: [Nature Chemistry] (Ref. 78), copyright 2013.

Macrocycle **114**[83] is a nearly planar 24π-electron antiaromatic molecule. It contains three rigid naphthobipyrrole subunits that are linked through methylene bridges. Upon protonation with hydrogen halides (HX), the neutral **114** was reduced to a formal 25π-electron radical dication species **118** via a proton-coupled electron transfer[84] process. In the case of HI, further reduction produced a 26π-electron aromatic cation **116** that can also be obtained independently using the more classic reductant. Upon deprotonation, the aromatic cation **118** spontaneously reverted to the neutral 24π-electron species **114** (Fig. 16 a). This was reflected in the UV-Vis-NIR absorption spectra, in which **114** showed a broad Soret-like band at 462 nm, whereas **118** showed a redshifted Soret-like band at 562 nm with two weak Q-like bands at 784 and 1081 nm. While aromatic **116** exhibits a sharp Soret band at 612 nm accompanied with three Q bands at 720, 802 and 888 nm (Fig. 16 b). Due to the ability to interconvert between three well-defined oxidation states, **114** may find application in the creation of switchable electronic materials.

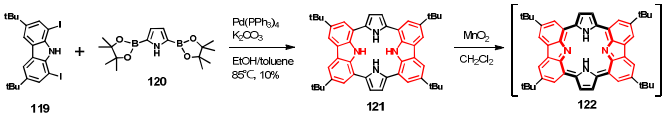

Scheme 21 Synthesis of carbazole-containing porphyrinoids **121** and **122**.

Carbazole-based materials have been extensively studied due to their high emission, electron conducting and chemically stable properties.[85, 86] Müllen *et al* successfully introduced two carbazole subunits into a porphyrin skeleton **121**[87] via a one-pot Suzuki coupling reaction of **119** and **120** (Scheme 21). The UV absorption of **121** showed two local maxima at 307 nm and 400 nm, which is typical for nonaromatic porphyrin system. Macrocycle**121** also exhibited blue emission at 427 nm with high quantum yield (Φ_f = 0.68, λ_{ex} = 349 nm). Interestingly, upon stepwise oxidation with MnO_2, three new Q-like bands arose at 846 nm, 945 nm and 1076 nm. The supposed structure of oxidized product was **122**, which is an 18π aromatic macrocycle. However, it was difficult to isolate **122** due to its poor stability. The palladium-catalyzed cross coupling method proved to be a new and efficient synthetic protocol to construct novel carbazole-containing porphyrinoids.[88]

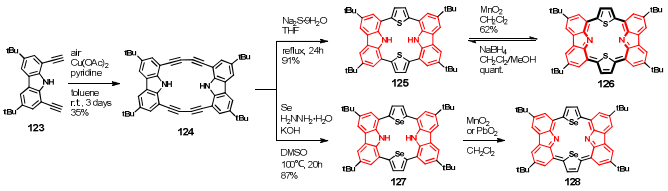

Scheme 22 Synthesis of carbazole-containing porphyrinoids **125-128**.

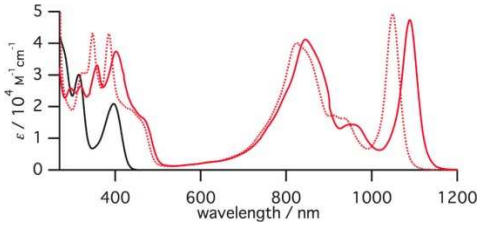

Fig. 17 UV-Vis absorption spectra in CH_2Cl_2 (black line: **127**, red dotted line: **126**, red line: **128**). Reproduced with permission from Ref. 85. Copyright 2013 American Chemical Society.

A multi-step cyclization strategy to incorporate carbazole into a core-modified porphyrin was reported by Maeda and Osuka *et al*. Macrocycle **124** was obtained by a Glaser coupling reaction from 1,8-diethynylcarbazole **123**. The thiophene and selenophene moieties in porphyrins **125**[89] and **127**[90] were generated in situ via the reaction of **124** with Na_2S and Se under proper conditions, respectively (Scheme 22). Both **125** and **127** are nonaromatic molecules with absorption under 500 nm. Upon oxidation with MnO_2, stable aromatic macrocycles **126**[89] and **128**[90] were obtained, each of which exhibited three Q-like absorption bands at 845, 934, 1049 nm and 845, 952, 1089 nm, respectively (Fig. 17). This multiple annulation protocol efficiently expanded the porphyrin synthetic methods compared to the general acid-catalyzed condensation-based synthesis. The carbazole-based porphyrins, which possess distinct aromaticity and expanded π conjugation, displayed remarkable intensified absorption that is well in the near infrared region.

3. Conclusion and outlook

In this review, we have summarized the remarkable progress in the field of synthesis and application of artificial porphyrinoids embedded with various functional building blocks. Various π-conjugated moieties with unique structural and electronic features have been incorporated into the porphyrin-like macrocycles through chemical modification. The macrocyclic porphyrin network offered a platform to embed functional building blocks which act as switches in the macrocycles to regulate the spacial conformation and aromaticity of porphyrinoids. Small five or six-membered rings such as cyclopentadiene and pyridine can be embedded into both tetra-unit and expanded porphyrin skeletons. Compared with pyrrole, these building blocks affect the π-conjugation pathway and coordination properties of porphyrins with tiny conformational perturbation. Linear oligomeric subunits can efficiently extend the conjugation of porphyrin, thus redshift their absorption into NIR region. Due to the rigid conformational features, porphyrinoids embedded with fused five/six-membered heterocycles adopt planar or near planar conformation with strong absorption in the NIR region. Furthermore, the unique local aromatic features of these building blocks affect the global aromatic properties of porphyrinoids.[63] It has been demonstrated that through rational design porphyrinoids embedded with functional building blocks exhibit many promising properties such as redox interconversion, unique metal coordination ability, aromatic switching, strong NIR absorption and emission. As promising photoelectric functional molecules, their application for photodynamic therapy, photovoltaics, molecular switch and non-linear optics need to be investigated deeply in the future. This review introduced an efficient strategy for tuning the structural and electronic properties of porphyrinoids, further researches on the incorporation of stimuli-responsive (redox, pH, light) building blocks into macrocyclic network to form switchable porphyrinoids are highly desirable.

Acknowledgements

Financial support was provided by the Major State Basic Research Development Program of China (Grant Nos. 2013CB922101 & 2011CB808704), the National Natural Science Foundation of China (No. 21371090), and the Natural Science Foundation of Jiangsu Province (BK20130054).

Notes and references

State Key Laboratory of Coordination Chemistry
School of Chemistry and Chemical Engineering
Nanjing University, Nanjing, 210093 (P. R. China)
E-mail: zshen@nju.edu.cn

Electronic Supplementary Information (ESI) available: [details of any supplementary information available should be included here]. See DOI: 10.1039/b000000x/

1 in *The Porphyrin Handbook*, eds. K. M. Kadish, K. M. Smith and R. Guilard, Academic Press, San Diego, 2000, vol. 6.
2 in *Handbook of Porphyrin Science*, eds. K. M. Kadish, K. M. Smith and R. Guilard, World Scientific Publishing, Singapore, 2010, vol. 1-25.
3 S. Mathew, A. Yella, P. Gao, R. Humphry-Baker, F. E. CurchodBasile, N. Ashari-Astani, I. Tavernelli, U. Rothlisberger, K. NazeeruddinMd and M. Grätzel, *Nat Chem*, 2014, **6**, 242-247.
4 Z.-L. Xue, Z. Shen, J. Mack, D. Kuzuhara, H. Yamada, T. Okujima, N. Ono, X.-Z. You and N. Kobayashi, *J. Am. Chem. Soc.*, 2008, **130**, 16478-16479.
5 A. Jasat and D. Dolphin, *Chem. Rev.*, 1997, **97**, 2267-2340.
6 J. L. Sessler and D. Seidel, *Angew. Chem. Int. Ed.*, 2003, **42**, 5134-5175.
7 J.-Y. Shin, K. S. Kim, M.-C. Yoon, J. M. Lim, Z. S. Yoon, A. Osuka and D. Kim, *Chem. Soc. Rev.*, 2010, **39**, 2751-2767.
8 H. Furuta, T. Asano and T. Ogawa, *J. Am. Chem. Soc.*, 1994, **116**, 767-768.
9 P. J. Chmielewski, L. Latos-Grażyński, K. Rachlewicz and T. Glowiak, *Angew. Chem. Int. Ed. Engl.*, 1994, **33**, 779-781.
10 D. Sanchez-Garcia and J. L. Sessler, *Chem. Soc. Rev.*, 2008, **37**, 215-232.
11 L. Latos-Grazynski, J. Lisowski, M. M. Olmstead and A. L. Balch, *J. Am. Chem. Soc.*, 1987, **109**, 4428-4429.
12 M. Stępień, N. Sprutta and L. Latos-Grażyński, *Angew. Chem. Int. Ed.*, 2011, **50**, 4288-4340.
13 S. Saito and A. Osuka, *Angew. Chem. Int. Ed.*, 2011, **50**, 4342-4373.

14 J. S. Lindsey, I. C. Schreiman, H. C. Hsu, P. C. Kearney and A. M. Marguerettaz, *J. Org. Chem.*, 1987, **52**, 827-836.
15 A. Ulman and J. Manassen, *J. Am. Chem. Soc.*, 1975, **97**, 6540-6544.
16 M. J. Broadhurst, R. Grigg and A. W. Johnson, *J. Chem. Soc. C*, 1971, 3681-3690.
17 P.-Y. Heo, K. Shin and C.-H. Lee, *Tetrahedron Lett.*, 1996, **37**, 197-200.
18 G. P. Arsenault, E. Bullock and S. F. MacDonald, *J. Am. Chem. Soc.*, 1960, **82**, 4384-4389.
19 C.-H. Lee and W.-S. Cho, *Tetrahedron Lett.*, 1999, **40**, 8879-8882.
20 M. Toganoh and H. Furuta, *Chem. Commun.*, 2012, **48**, 937-954.
21 I. Gupta and M. Ravikanth, *Coord. Chem. Rev.*, 2006, **250**, 468-518.
22 T. D. Lash, *Eur. J. Org. Chem.*, 2007, **2007**, 5461-5481.
23 L. Arnold and K. Müllen, *J. Porphyrins Phthalocyanines*, 2011, **15**, 757-779.
24 A. Berlicka, P. Dutka, L. Szterenberg and L. Latos-Grażyński, *Angew. Chem. Int. Ed.*, 2014, **53**, 4885-4889.
25 T. D. Lash, *Chem. - Asian J.*, 2014, **9**, 682-705.
26 J. Klingele, S. Dechert and F. Meyer, *Coord. Chem. Rev.*, 2009, **253**, 2698-2741.
27 S. Mori and A. Osuka, *J. Am. Chem. Soc.*, 2005, **127**, 8030-8031.
28 L. K. Frensch, K. Pröpper, M. John, S. Demeshko, C. Brückner and F. Meyer, *Angew. Chem. Int. Ed.*, 2011, **50**, 1420-1424.
29 L. K. Blusch, K. E. Craigo, V. Martin-Diaconescu, A. B. McQuarters, E. Bill, S. Dechert, S. DeBeer, N. Lehnert and F. Meyer, *J. Am. Chem. Soc.*, 2013, **135**, 13892-13899.
30 A. B. Descalzo, H.-J. Xu, Z.-L. Xue, K. Hoffmann, Z. Shen, M. G. Weller, X.-Z. You and K. Rurack, *Org. Lett.*, 2008, **10**, 1581-1584.
31 H.-J. Xu, J. Mack, A. B. Descalzo, Z. Shen, N. Kobayashi, X.-Z. You and K. Rurack, *Chem. - Eur. J.*, 2011, **17**, 8965-8983.
32 H.-J. Xu, J. Mack, D. Wu, Z.-L. Xue, A. B. Descalzo, K. Rurack, N. Kobayashi and Z. Shen, *Chem. - Eur. J.*, 2012, **18**, 16844-16867.
33 X. Zhang, H. Xu, Y. Shen, Y. Wang, Z. Shen, Q. Zeng and C. Wang, *PCCP*, 2013, **15**, 12510-12515.
34 J. Roncali, *Chem. Rev.*, 1997, **97**, 173-206.
35 Y. Shimizu, Z. Shen, S. Ito, H. Uno, J. Daub and N. Ono, *Tetrahedron Lett.*, 2002, **43**, 8485-8488.
36 Y. Shimizu, Z. Shen, T. Okujima, H. Uno and N. Ono, *Chem. Commun.*, 2004, 374-375.
37 Y. Matano, M. Nakashima, T. Nakabuchi, H. Imahori, S. Fujishige and H. Nakano, *Org. Lett.*, 2008, **10**, 553-556.
38 T. Nakabuchi, M. Nakashima, S. Fujishige, H. Nakano, Y. Matano and H. Imahori, *J. Org. Chem.*, 2010, **75**, 375-389.
39 T. Nakabuchi, Y. Matano and H. Imahori, *Org. Lett.*, 2010, **12**, 1112-1115.
40 C. Romero-Nieto and T. Baumgartner, *Synlett*, 2013, **24**, 920-937.
41 P. v. R. Schleyer, C. Maerker, A. Dransfeld, H. Jiao and N. J. R. v. E. Hommes, *J. Am. Chem. Soc.*, 1996, **118**, 6317-6318.
42 Z. Chen, C. S. Wannere, C. Corminboeuf, R. Puchta and P. v. R. Schleyer, *Chem. Rev.*, 2005, **105**, 3842-3888.
43 Y. Matano, T. Nakabuchi, S. Fujishige, H. Nakano and H. Imahori, *J. Am. Chem. Soc.*, 2008, **130**, 16446-16447.
44 J. Skonieczny, L. Latos-Grażyński and L. Szterenberg, *Chem. - Eur. J.*, 2008, **14**, 4861-4874.
45 J. Skonieczny, L. Latos-Grazynski and L. Szterenberg, *Org. Biomol. Chem.*, 2012, **10**, 3463-3471.
46 M. Stępień and L. Latos-Grażyński, *Chem. - Eur. J.*, 2001, **7**, 5113-5117.
47 K. Berlin and E. Breitmaier, *Angew. Chem. Int. Ed. Engl.*, 1994, **33**, 1246-1247.
48 M. Stępień and L. Latos-Grażyński, *J. Am. Chem. Soc.*, 2002, **124**, 3838-3839.
49 T. D. Lash, A. M. Young, J. M. Rasmussen and G. M. Ferrence, *J. Org. Chem.*, 2011, **76**, 5636-5651.
50 B. Szyszko, K. Kupietz, L. Szterenberg and L. Latos-Grażyński, *Chem. - Eur. J.*, 2014, **20**, 1376-1382.
51 I. T. Ho, Z. Zhang, M. Ishida, V. M. Lynch, W.-Y. Cha, Y. M. Sung, D. Kim and J. L. Sessler, *J. Am. Chem. Soc.*, 2014, **136**, 4281-4286.
52 R. Herges and D. Geuenich, *J. Phys. Chem. A*, 2001, **105**, 3214-3220.
53 D. Geuenich, K. Hess, F. Köhler and R. Herges, *Chem. Rev.*, 2005, **105**, 3758-3772.
54 A. Srinivasan, V. M. Reddy, S. J. Narayanan, B. Sridevi, S. K. Pushpan, M. Ravikumar and T. K. Chandrashekar, *Angew. Chem. Int. Ed. Engl.*, 1997, **36**, 2598-2601.
55 D. Wu, A. B. Descalzo, F. Weik, F. Emmerling, Z. Shen, X.-Z. You and K. Rurack, *Angew. Chem. Int. Ed.*, 2008, **47**, 193-197.
56 J. Tian, L. Ding, H.-J. Xu, Z. Shen, H. Ju, L. Jia, L. Bao and J.-S. Yu, *J. Am. Chem. Soc.*, 2013, **135**, 18850-18858.
57 H. Rath, V. Prabhuraja, T. K. Chandrashekar, A. Nag, D. Goswami and B. S. Joshi, *Org. Lett.*, 2006, **8**, 2325-2328.
58 T. Y. Gopalakrishna, J. S. Reddy and V. G. Anand, *Angew. Chem. Int. Ed.*, 2013, **52**, 1763-1767.
59 T. Y. Gopalakrishna and V. G. Anand, *Angew. Chem. Int. Ed.*, 2014, **53**, 6678-6682.
60 L. N. Lucas, J. van Esch, R. M. Kellogg and B. L. Feringa, *Chem. Commun.*, 1998, 2313-2314.
61 S. Lee, Y. You, K. Ohkubo, S. Fukuzumi and W. Nam, *Angew. Chem. Int. Ed.*, 2012, **51**, 13154-13158.
62 Z. Zhou, Y. Chang, S. Shimizu, J. Mack, C. Schütt, R. Herges, Z. Shen and N. Kobayashi, *Angew. Chem. Int. Ed.*, 2014, **53**, 6563-6567.
63 Y. Nakagami, R. Sekine and J.-i. Aihara, *Org. Biomol. Chem.*, 2012, **10**, 5219-5229.
64 I. Simkowa, L. Latos-Grażyński and M. Stępień, *Angew. Chem. Int. Ed.*, 2010, **49**, 7665-7669.
65 I. Grocka, L. Latos-Grażyński and M. Stępień, *Angew. Chem. Int. Ed.*, 2013, **52**, 1044-1048.
66 Y. Chang, H. Chen, Z. Zhou, Y. Zhang, C. Schütt, R. Herges and Z. Shen, *Angew. Chem. Int. Ed.*, 2012, **51**, 12801-12805.
67 J. L. Sessler, M. R. Johnson and V. Lynch, *J. Org. Chem.*, 1987, **52**, 4394-4397.
68 H. Rath, A. Mallick, T. Ghosh and A. Kalita, *Chem. Commun.*, 2014, **50**, 9094-9096.
69 F. Cicoira, C. Santato, M. Melucci, L. Favaretto, M. Gazzano, M. Muccini and G. Barbarella, *Adv. Mater.*, 2006, **18**, 169-174.
70 K. Lu, C.-a. Di, H. Xi, Y. Liu, G. Yu, W. Qiu, H. Zhang, X. Gao, Y. Liu, T. Qi, C. Du and D. Zhu, *J. Mater. Chem.*, 2008, **18**, 3426-3432.
71 T. K. Chandrashekar, V. Prabhuraja, S. Gokulnath, R. Sabarinathan and A. Srinivasan, *Chem. Commun.*, 2010, **46**, 5915-5917.
72 G. Karthik, A. Srinivasan and T. K. Chandrashekar, *Org. Lett.*, 2014, **16**, 3472-3475.
73 G. Karthik, J. M. Lim, A. Srinivasan, C. H. Suresh, D. Kim and T. K. Chandrashekar, *Chem. - Eur. J.*, 2013, **19**, 17011-17020.

74 M. Ishida, Y. Naruta and F. Tani, *Angew. Chem. Int. Ed.*, 2010, **49**, 91-94.
75 E.-K. Sim, S.-D. Jeong, D.-W. Yoon, S.-J. Hong, Y. Kang and C.-H. Lee, *Org. Lett.*, 2006, **8**, 3355-3358.
76 M. Ishida, S. Karasawa, H. Uno, F. Tani and Y. Naruta, *Angew. Chem. Int. Ed.*, 2010, **49**, 5906-5909.
77 P. K. Panda, Y.-J. Kang and C.-H. Lee, *Angew. Chem. Int. Ed.*, 2005, **44**, 4053-4055.
78 D.-G. Cho, P. Plitt, S. K. Kim, V. Lynch, S.-J. Hong, C.-H. Lee and J. L. Sessler, *J. Am. Chem. Soc.*, 2008, **130**, 10502-10503.
79 S.-Y. Kee, J. M. Lim, S.-J. Kim, J. Yoo, J.-S. Park, T. Sarma, V. M. Lynch, P. K. Panda, J. L. Sessler, D. Kim and C.-H. Lee, *Chem. Commun.*, 2011, **47**, 6813-6815.
80 T. Sarma and P. K. Panda, *Chem. - Eur. J.*, 2011, **17**, 13987-13991.
81 V. V. Roznyatovskiy, J. M. Lim, V. M. Lynch, B. S. Lee, D. Kim and J. L. Sessler, *Org. Lett.*, 2011, **13**, 5620-5623.
82 D. Swain, P. T. Anusha, T. Sarma, P. K. Panda and S. Venugopal Rao, *Chem. Phys. Lett.*, 2013, **580**, 73-77.
83 M. Ishida, S.-J. Kim, C. Preihs, K. Ohkubo, J. M. Lim, B. S. Lee, J. S. Park, V. M. Lynch, V. V. Roznyatovskiy, T. Sarma, P. K. Panda, C.-H. Lee, S. Fukuzumi, D. Kim and J. L. Sessler, *Nat Chem*, 2013, **5**, 15-20.
84 D. R. Weinberg, C. J. Gagliardi, J. F. Hull, C. F. Murphy, C. A. Kent, B. C. Westlake, A. Paul, D. H. Ess, D. G. McCafferty and T. J. Meyer, *Chem. Rev.*, 2012, **112**, 4016-4093.
85 J.-F. Morin and M. Leclerc, *Macromolecules*, 2002, **35**, 8413-8417.
86 N. Blouin, A. Michaud and M. Leclerc, *Adv. Mater.*, 2007, **19**, 2295-2300.
87 L. Arnold, M. Baumgarten and K. Mullen, *Chem. Commun.*, 2012, **48**, 9640-9642.
88 M. Masuda and C. Maeda, *Chem. - Eur. J.*, 2013, **19**, 2971-2975.
89 C. Maeda, T. Yoneda, N. Aratani, M.-C. Yoon, J. M. Lim, D. Kim, N. Yoshioka and A. Osuka, *Angew. Chem. Int. Ed.*, 2011, **50**, 5691-5694.
90 M. Masuda, C. Maeda and N. Yoshioka, *Org. Lett.*, 2013, **15**, 578-581.

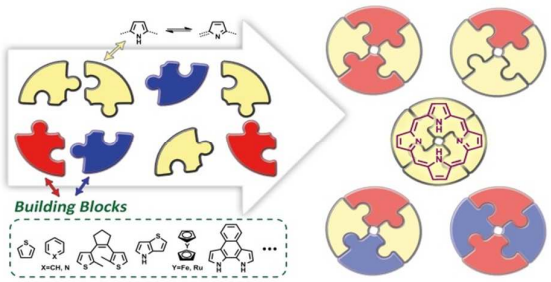

The synthesis and applications of artificial porphyrinoids containing various functional building blocks by replacements of pyrrole subunit have been summarized.